Consistency of heterogeneous synchronization patterns in complex weighted networks

D. Malagarriga, A. E. P. Villa, J. Garcia-Ojalvo, and A. J. Pons

Citation: Chaos **27**, 031102 (2017); doi: 10.1063/1.4977972
View online: http://dx.doi.org/10.1063/1.4977972
View Table of Contents: http://aip.scitation.org/toc/cha/27/3
Published by the American Institute of Physics

Consistency of heterogeneous synchronization patterns in complex weighted networks

D. Malagarriga,[1,2,a] A. E. P. Villa,[3] J. Garcia-Ojalvo,[4] and A. J. Pons[1]
[1]*Departament de Física, Universitat Politècnica de Catalunya. Edifici Gaia, Rambla Sant Nebridi 22, 08222 Terrassa, Spain*
[2]*Centre for Genomic Regulation (CRG). Barcelona Biomedical Research Park (PRBB), Dr. Aiguader 88, 08003 Barcelona, Spain*
[3]*Neuroheuristic Research Group, Faculty of Business and Economics, University of Lausanne. CH-1015 Lausanne, Switzerland*
[4]*Department of Experimental and Health Sciences, Universitat Pompeu Fabra, Barcelona Biomedical Research Park (PRBB), Dr. Aiguader 88, 08003 Barcelona, Spain*

(Received 22 January 2017; accepted 20 February 2017; published online 9 March 2017)

Synchronization within the dynamical nodes of a complex network is usually considered homogeneous through all the nodes. Here we show, in contrast, that subsets of interacting oscillators may synchronize in different ways within a single network. This diversity of synchronization patterns is promoted by increasing the heterogeneous distribution of coupling weights and/or asymmetries in small networks. We also analyze *consistency*, defined as the persistence of coexistent synchronization patterns regardless of the initial conditions. Our results show that complex weighted networks display richer consistency than regular networks, suggesting why certain functional network topologies are often constructed when experimental data are analyzed. © *2017 Author(s). All article content, except where otherwise noted, is licensed under a Creative Commons Attribution (CC BY) license (http://creativecommons.org/licenses/by/4.0/).* [http://dx.doi.org/10.1063/1.4977972]

Dynamical systems may synchronize in several ways, at the same time, when they are coupled in a single complex network. Examples of this diversity of synchronization patterns may be found in research fields as diverse as neuroscience, climate networks, or ecosystems. Here we report the conditions required to obtain coexisting synchronizations in arrangements of interacting chaotic oscillators, and relate these conditions to the distribution of coupling weights and asymmetries in complex networks. We also analyze the conditions required for a high statistical occurrence of the same synchronization patterns, regardless of the oscillators' initial conditions. Our results show that these persistent synchronization patterns are statistically more frequent in complex weighted networks than in regular ones, explaining why certain functional network topologies are often retrieved from experimental data. Besides, our results suggest that considering both the different coexisting synchronizations and also their statistics may result in a richer understanding of the relations between functional and structural networks of oscillators.

I. INTRODUCTION

Certain dynamical systems, which display oscillatory behavior in isolation, may display a wide repertoire of dynamical evolutions due to the coupling with their neighbors when embedded in networks of similar complex items.[1] The relationship between network dynamics and structure in this type of systems is therefore a fundamental question in network science. For instance, the interaction of rhythmic elements may entail an adjustment of their oscillatory dynamics to finally end up in a state of (dynamical) *agreement* or *synchronization*.[2–4] When coupling is strong, the oscillators in a network usually synchronize in a particular collective oscillatory behavior. However, for more moderate coupling intensity, this relationship may also be inhomogeneous, i.e., certain oscillators may synchronize whereas others may not.[5–10] The specific patterns of synchronization, thus, provide information about the underlying couplings between the dynamical elements forming the network. Hence, a better characterization of the system can be achieved by analyzing all the synchronization relationships within a network instead of analyzing a single synchronization relationship. This type of characterization might be of crucial importance when the details of the contacts between the oscillators are not available.

In the past, studies of the synchronization patterns in networks of oscillators were mainly aimed at describing the conditions associated with the emergence of specific synchronization patterns in all the nodes.[11] In the particular case of complex networks of coupled nonlinear oscillators, recent studies have provided evidence that it is possible to identify an appropriate interaction regime that allows to collect measured data to infer the underlying network structure based on time-series statistical similarity analysis[12] or connectivity stability analysis.[13] In real-life systems, such as ecological networks,[14] brain oscillations,[15–18] or climate interactions,[19] various types of complex synchronized dynamics have been observed to coexist in a single network. Therefore, such a diversity in dynamical relationships between the nodes

[a]Author to whom correspondence should be addressed. Electronic mail: daniel.malagarriga@upc.edu

 © Author(s) 2017.

endows a network with stability, flexibility, and robustness against perturbations.[20]

The present work reveals that several types of stable synchronization patterns may coexist depending on the topology and on the distribution of coupling strengths within a network. Besides, the capacity of a network to display the same heterogeneous synchronization pattern regardless of the initial conditions, or *consistency*, is also investigated. Such a property, observed in some type of networks, allows to retrieve network structure from its dynamics in a more reliable way than using single synchronization patterns.

II. COEXISTENCE OF SYNCHRONIZATIONS

Consider two n-dimensional dynamical systems, $\mathbf{x}$ and $\mathbf{y}$, whose temporal evolutions are generally defined by $\dot{\mathbf{x}}(t) = \mathbf{F}(\mathbf{x}(t))$, $\dot{\mathbf{y}}(t) = \mathbf{G}(\mathbf{y}(t))$ in isolation. Assuming a bidirectional coupling scheme, the coupled system reads:

$$\begin{aligned}\dot{\mathbf{x}}(t) &= \mathbf{F}(\mathbf{x}(t)) + \hat{\mathbf{C}}(\mathbf{y}(t) - \mathbf{x}(t)),\\ \dot{\mathbf{y}}(t) &= \mathbf{G}(\mathbf{y}(t)) + \hat{\mathbf{C}}(\mathbf{x}(t) - \mathbf{y}(t)).\end{aligned} \tag{1}$$

Here, $\mathbf{x}(t)$ and $\mathbf{y}(t)$ are the n-dimensional state vectors of the systems, $\mathbf{F}$ and $\mathbf{G}$ are their corresponding vector fields, and $\hat{\mathbf{C}}$ is a $n \times n$ matrix that provides the coupling characteristics between the sub-systems. When coupling is strong enough and these dynamical systems are oscillators, the synchronization relationships that can be established between them can be categorized in four types (see time traces in Fig. 1):[22,23]

- Phase synchronization (PS) appears if the functional relationship between the dynamics of two oscillators preserves a bounded phase difference,[24] with their amplitudes being largely uncorrelated. This can be exemplified by the relationship $|n\phi_1 - m\phi_2| < \text{const}$, with n and m being integer numbers which define the ratio between the phases $\phi_{1,2}$ of the two coupled oscillators.
- Generalized synchronization (GS) is observed if a complex functional relationship is established between the oscillators,[25] e.g., $\mathbf{y}(t) = H[\mathbf{x}(t)]$, where $H[\mathbf{x}(t)]$ can take any form other than identity. It can be thought to be a generalization of complete synchronization (CS) for non-identical oscillators.
- Lag synchronization (LS) appears when the amplitude correlation is high while at the same time there is a time shift in the dynamics of the oscillators,[26] $\mathbf{y}(t) = \mathbf{x}(t - \tau)$, with τ being a lag time.
- Complete synchronization (CS) is observed when the coupled oscillators are identical or almost identical,[27] and $\mathbf{x}(t) = \mathbf{y}(t)$ for a sufficiently large coupling strength $\hat{\mathbf{C}}$.

There are several analysis techniques that can be used to assess the emergence of each of the mentioned synchronization motifs. Here, three of them are combined: cross-correlation (CC), Phase-Locking Value (PLV), and the Nearest-Neighbor Method (NNM). CC computes the lagged similarity or sliding

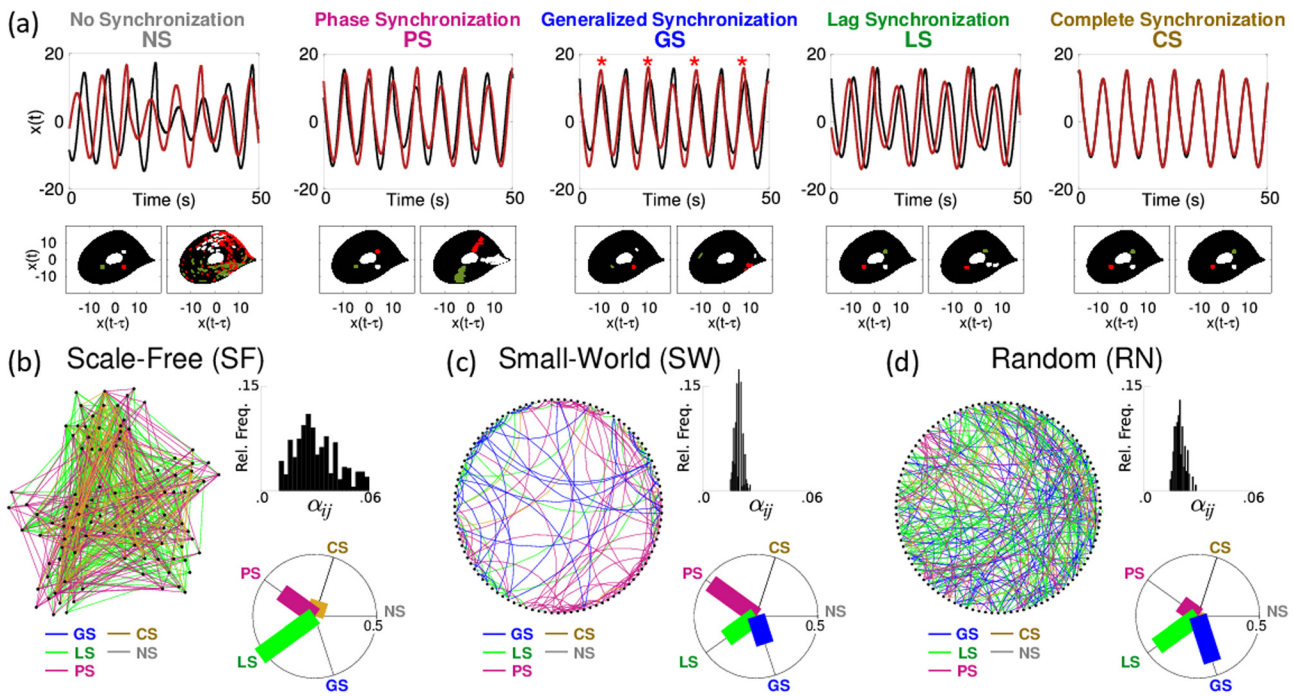

FIG. 1. Heterogeneous synchronization patterns in complex weighted networks. (a) Examples of synchronization patterns (no synchronization NS, phase synchronization PS, generalized synchronization GS, lag synchronization LS, and complete synchronization CS) displayed by bidirectionally coupled Rössler oscillators. The upper panels show examples of $x_i(t)$ time traces for each synchronization pattern and the lower panels show examples of the corresponding delay-embedding plot.[21] τ is the delay time for maximal cross-correlation in LS and PS. Examples of (b) a scale-free (SF) network ($K = 0.4$), (c) small-world (SW) network with low rewiring probability ($K = 0.1$), and (D) random (RN) ($K = 0.1$) of coupled Rössler oscillators displaying heterogeneous synchronization patterns. All networks have $N = 100$ nodes. K is a global coupling parameter controlling the maximum coupling strength between two adjacent nodes (see Eq. (3)). For each type of network the right panels show the distribution of the coupling strengths α_{ij} between pairs of nodes (upper panel) and the distribution of the synchronization patterns (polar histogram, lower panel). Each link is color-coded so as to show which synchronization pattern is displayed by each pair of oscillators within the network (NS, PS, GS, LS, CS see left bottom legend).

dot product between two signals, which provides a notion of the amplitude resemblance over time. Therefore, it allows to identify whether CS or LS is established between two time traces. On the other hand, PLV makes use of the Hilbert transform of a signal to retrieve a phase ϕ and compute the time evolution of the difference in the phases of two oscillators, i.e., $\phi_1(t) - \phi_2(t)$,[28] as

$$PLV_t = \frac{1}{N}\left|\sum_{n=1}^{N}\langle e^{i\Delta\phi_{12}(t,n)}\rangle_t\right|, \tag{2}$$

where $\Delta\phi_{12}(t,n)$ is the evolution of the difference between the phases of oscillators 1 and 2, N is the number of trials, and $\langle\ldots\rangle_t$ denotes temporal average. This measure can assess, when combined with low CC, the emergence of PS between two oscillators. Finally, the NNM takes points in the phase space of each oscillator and characterizes their relative evolution.[27] This method allows to visualize and exemplify each synchronization motif as well as to identify the emergence of generalized synchronization between two oscillators[21] (see examples in Fig. 1(a), lower panels). In order to establish thresholds for each synchronized state we computed an average distance d of the images $\mathbf{u}^{\mathbf{k},\mathbf{kn}}$ of the nearest neighbors $\mathbf{x}^{\mathbf{k},\mathbf{kn}}$ of two coupled oscillators as performed in Ref. 21. We took the reported values of d that indicate the onset of each synchronization and compared these values with our CC and PLV calculations in the same situation. Thanks to this, we established thresholds ξ_i for computing each synchronization pattern in the particular case of Rössler oscillators: PS entails $\xi_{PLV} \geq 0.9$ and $\xi_{CC} \leq 0.5$ with lag 0, GS can be identified if $\xi_{PLV} \geq 0.9$ and $\xi_{CC} \geq 0.9$ with $\text{lag} \geq 1$, LS is present if $\xi_{PLV} \geq 0.9$ and $\xi_{CC} \geq 0.9$ with $0 \leq \text{lag} < 1$, and finally CS emerges if $\xi_{PLV} \geq 0.9$ and $\xi_{CC} \geq 0.9$ with $\text{lag} = 0$. With this set of analysis techniques, here, the dynamics of networks of coupled Rössler oscillators[29] arranged in complex weighted topologies—random (RN),[30] small-world (SW),[31] and scale-free (SF)[32]—are studied.

The dynamics of each node i follow the 3-dimensional Rössler equations, which read

$$\begin{aligned}\dot{x}_i &= -\omega_i y_i - z_i + K\sum_{j=1,j\neq i}^{N_{neigh}}\alpha_{ij}(x_j - x_i),\\ \dot{y}_i &= \omega_i x_i + a y_i,\\ \dot{z}_i &= p + z_i(x_i - c),\end{aligned} \tag{3}$$

where K is a global parameter controlling the maximum coupling strength between two nodes and ω_i is the natural frequency of the node i, which is normally distributed with average $\langle\omega\rangle = 1$ and standard deviation $\sigma_\omega = 0.02$. An isolated node with Rössler dynamics can display periodic, quasi-periodic, or chaotic dynamics, and we choose $a = 0.15$, $p = 0.2$, and $c = 10$ to set the oscillators into a chaotic regime.[27] The coupling weights are set to depend on the number of neighbors of each node, if not specified otherwise, as

$$\alpha_{ij} = \frac{1}{\sqrt{\deg(v_i)\deg(v_j)}}, \tag{4}$$

for $i \neq j$, where $\deg(v_i)$, $\deg(v_j)$ are the degrees (number of coupled neighbors) of two coupled nodes v_i, v_j.

Figures 1(b)–1(d) show the distribution of synchronizations in three prototypical networks (composed of $N = 100$ nodes), namely, SF, SW, and RN, alongside with their weight distributions (relative frequency of α_{ij}) and the distribution of synchronizations within each network. All three networks are located in a region of the coupling parameter space which allows a complex distribution of synchronizations, in between a non-synchronized and an all-synchronized network scenario. We call this type of behavior *coexistence* of synchronization patterns. In this sense, the SF network shows clusters of PS, LS, and CS, and SW and RN networks show clusters of PS, GS, and LS, allowing for functional relationships between the oscillators. However, such distribution is very sensitive to the coupling characteristics and the underlying topology. Here, we show results for small and medium size networks. Naturally, the question of how our results scale with the network size is raised. The results shown here and other not shown indicate that what is relevant for the presence or absence of coexistence of synchronizations in a network is the distribution of couplings and not so much the size of the network. Further studies will have to explore, in detail, the dependence of coexistence (and consistence) of synchronization patterns with the network size. A proper characterization of the phenomenon requires the detailed analysis of the interaction of the oscillators' dynamics and the networks they are embedded in.

III. CONSISTENCY OF SYNCHRONIZATIONS

The heterogeneous synchronization motifs that emerge in complex networks are an excellent probe to detect the functional connectivity between the oscillators in a network. Besides, if these motifs are dynamically stable, synchronized states that show up recurrently when changing initial conditions might be identified, thus becoming an *invariant* feature of the dynamics of the network. We are going to show that the attractor's basin for specific coexistent synchronization patterns will depend on the topology of the network. So, in this section, we explore the conditions for the *consistency* of synchronization patterns which we define as the persistence of the coexistent synchronization patterns regardless of the initial conditions.

A first example of coexistence of synchronizations is studied in a very simple weighted network formed by two pairs of nodes connected bidirectionally with a fifth node (see Fig. 2(a), Eq. (3)). The oscillators only differ on the frequencies, ω_i, which are the following: $\omega_1 = 0.930$, $\omega_2 = 0.967$, $\omega_3 = 0.990$, $\omega_4 = 0.950$, and $\omega_5 = 0.970$. After fixing α_{12} and α_{34}, the synchronization coexistence within the network can be changed by increasing the bidirectional coupling α_c with the central node. Notice that the synchronization states evolve without changing $\alpha_{1,2}$ and $\alpha_{3,4}$ (the peripheral nodes' coupling strengths).

Since non-identical oscillators are taken into account, there is no global synchronization manifold and, therefore, an *analytical* stability analysis of the whole system cannot be performed. However, the evolution of the coexistence of synchronized states in terms of α_c may be tracked numerically

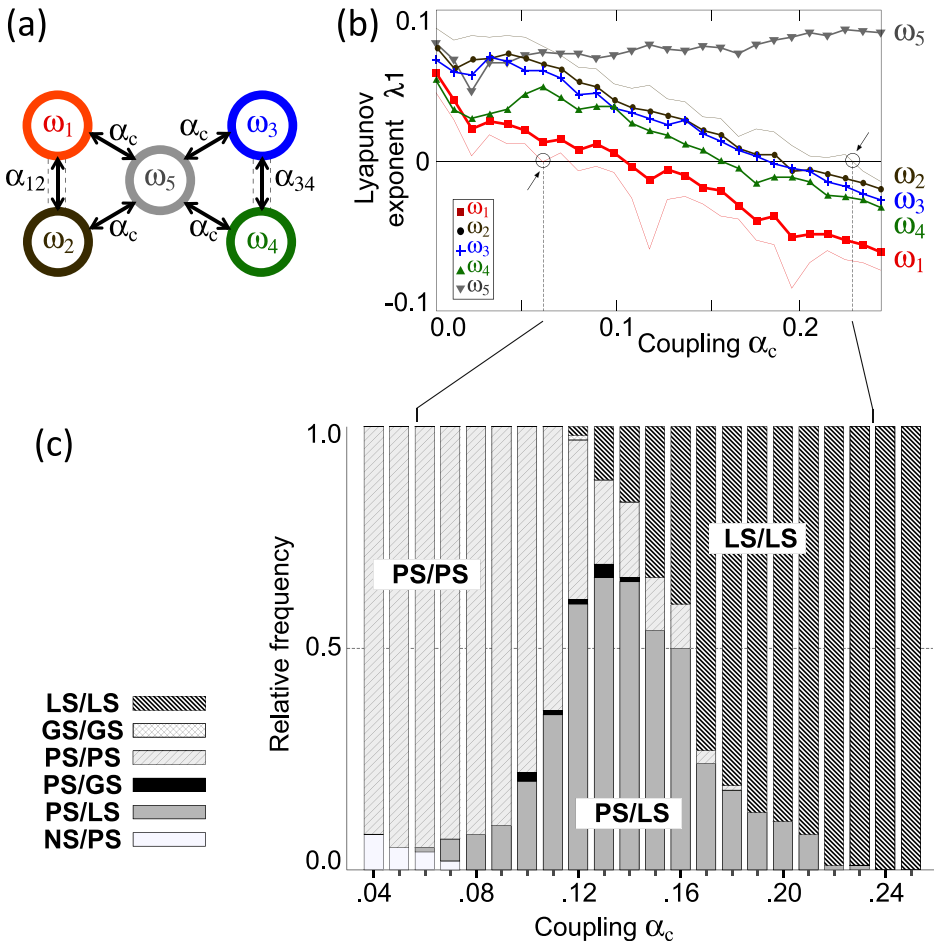

FIG. 2. Dependence of the coexistence of synchronization patterns on the Lyapunov Exponents. (a) Simple weighted network formed by two pairs of peripheral nodes connected to a central node. The couplings between peripheral node pairs are $\alpha_{12}=0.05$ and $\alpha_{34}=0.03$. (b) For each node dynamics the curves show the mean value (computed over 100 runs with random initial conditions) of the maximum Lyapunov exponent ($\lambda 1$) as a function of the strength of coupling α_c of all nodes with the central node. The lowest thin curve corresponds to the lowest values of $\lambda 1$ for node ω_1 computed independently for each value of α_c. This curve crosses the zero line at $\alpha_c=0.06$, as indicated by an arrow and a vertical dotted line. The uppermost thin curve corresponds to the largest values of $\lambda 1$ for node ω_2. This curve crosses the zero line at $\alpha_c=0.23$, as indicated by an arrow and a vertical dotted line. (c) Histogram of the occurrences of the synchronized patterns for each peripheral node pair in the network (1–2 and 3–4). Notice that in the interval $\alpha_c \in [0.06, 0.23]$ several synchronization patterns may coexist for the same coupling α_c, depending only on the randomly chosen initial conditions.

by considering in detail the values of the *Conditional* Lyapunov Exponents (CLEs, $\lambda 1_{\omega_i}$)[21,27] when α_c changes (see Fig. 2(b)), indicating the onset of a different synchronization motifs. Lyapunov exponents are a measure that characterizes the stability or instability of the evolution of a dynamical system with respect to varying initial conditions or perturbations.

For two unidirectionally coupled oscillators, $\mathbf{x}(t)$ and $\mathbf{u}(t)$ of dimensions N_x and N_u, respectively, in which $\mathbf{x}(t)$ drives $\mathbf{u}(t)$, one can consider the presence of a time-dependent functional relationship

$$\mathbf{u}(t) = \mathbf{H}[\mathbf{x}(t)]. \tag{5}$$

The dynamics of this coupled drive-response system is characterized by the Lyapunov exponent spectra $\lambda_1^x \geq \lambda_2^x \geq \cdots \geq \lambda_{N_x}^x$ and $\lambda_1^u \geq \lambda_2^u \geq \cdots \geq \lambda_{N_u}^u$, with the latter being conditional Lyapunov exponents. In this sense, the rate of convergence or divergence of the trajectory of oscillator $\mathbf{u}$ towards the trajectory defined by oscillator $\mathbf{x}$ is given by λ_1^u: if $\lambda_1^u > 0$ the trajectories diverge, whereas if $\lambda_1^u < 0$ they converge.

Since throughout this manuscript a mutual coupling scheme is considered, Eq. (5) no longer holds for all time t, but rather its implicit form $\mathbf{H}[\mathbf{x}(t), \mathbf{u}(t)]=0$. However, locally (i.e., for $t^*-\delta<t<t^*+\delta$, with δ being infinitely small), the implicit function theorem[33] allows to write $\mathbf{x}(t^*)=\hat{\mathbf{H}}[\mathbf{u}(t^*)]$ or $\mathbf{u}(t^{**})=\tilde{\mathbf{H}}[\mathbf{x}(t^{**})]$, for other moments in time t. Therefore, without loss of generality, the spectrum of Lyapunov exponents can be computed in terms of the trajectory defined by one of the mutually coupled oscillators, either $\mathbf{u}$ or $\mathbf{x}$, as in the unidirectional coupling case. In what follows, the evolution of the flow of the trajectories of the coupled Rössler oscillators with respect to the trajectory defined by one of the oscillators in the networks is considered for small networks. This calculation allows to estimate whether such trajectory is attractive (i.e., neighboring oscillators converge to it and therefore synchronize) or repulsive (i.e., neighboring oscillators diverge from it and desynchronize in amplitude).

Figure 2(b) shows that, in terms of α_c, three different regions may be defined for the 5 (realization-averaged) largest CLEs, $\lambda 1_{\omega_i}$:

- In the first region ($0<\alpha_c\leq 0.06$) all the largest CLEs, are positive. The pairs 1–2 and 3–4 are mostly in PS. When increasing α_c in this region, peripheral nodes become PS with the central node until the first 0 crossing of $\lambda 1_{\omega_i}$ (light red line), which defines the onset for LS for pair 1–2 (vertical dashed line, first arrow, $\alpha_c=0.07$).
- The second region ($0.07\leq\alpha_c<0.23$, in between dashed lines) sets a cascade of coexistence of synchronization regimes, i.e., successive zero-crossings of CLEs, determine the onset of GS and LS between the nodes. Notice that the heterogenous pattern PS/LS is the most frequently observed. Pattern PS/GS was rare and pattern GS/LS was never observed.
- In the third region, after $\alpha_c=0.23$, there is the onset of LS for the whole network.

Figure 2(c) shows the histogram of the occurrence of each pair of synchronized states between nodes 1–2 or 3–4, computed using CC, PLV, and NNM: in the coexisting region, there exist extended α_c values for which pairs 1–2 and 3–4 are, simultaneously, in several different synchronized regimes, e.g., 1–2 are in LS meanwhile nodes 3–4 are in PS. Therefore, for this range of coupling α_c, several synchronized states can coexist in the network.

The cascade of zero-crossings of the CLEs, in terms of α_c can be expanded or squeezed by increasing or decreasing the symmetries of the system, and therefore the range of α_c values for which coexistence appears. For a completely symmetrical system, i.e., equal governing equations for all the nodes in a symmetric network, there are abrupt transitions to synchrony,[34] without coexistence. Symmetry can be broken in a controlled way by means of a parameter governing the dynamics (e.g., oscillatory frequency), a parameter responsible for the topological characteristics of the network (e.g., clustering), or both features. In such scenarios different motifs of synchronized dynamics may show up, but they are restricted to a tiny region of the parameter space and, hence, appear to be spurious. Here, symmetry is broken by adding mismatches between the frequencies of the oscillators and by increasing the heterogeneity of the nodes' degrees as well as the coupling values α_{ij}.

Figure 3(a) shows the motif studied previously, but with different coupling strengths between peripheral nodes; $\alpha_{1,2}$ is now one order of magnitude smaller than $\alpha_{3,4}$ (see caption of Fig. 3), making this motif more asymmetrical in terms of coupling strength. Again, the evolution of the CLEs, is tracked for increasing α_c values. First, for $\alpha_c = 0$, nodes 1–2 are in PS meanwhile nodes 3–4 are in GS—i.e., a coexistence situation. As can be seen in Fig. 3(a), for different initial conditions zero-crossings of CLEs, appear along an extended α_c value region. In this case, the coexistence region for peripheral nodes 1–2 and 3–4 spans from $\alpha_c = 0$ to $\alpha_c = 0.20$. The right panel in Fig. 3(a) shows a plot of the relative frequency of synchronizations found for each pair of nodes in the small motif for $\alpha_c = 0.04$ (three pointed star) and $\alpha_c = 0.18$ (dotted circle). In the first case, $\alpha_c = 0.04$, each pair in the network lays in the same synchronization state for any of the imposed initial conditions, whereas in the second case, $\alpha_c = 0.18$, many pairs display different synchronizations depending on the initial conditions. Consequently, the first case displays more *consistency* than the second case because the network shows the same coexistence pattern regardless of the initial conditions.

Figure 3(b) shows a more symmetric network, in terms of coupling strength α_c. Such relay configuration is less prone to synchronize for small coupling strengths and, therefore, larger α_c values are required to set synchronized states (see inset $\alpha_c = 0.18$). Fig. 3(b) lower right panel shows the relative frequency of synchronizations, with no large predominance of a single synchronization motif for a given pair of nodes. Therefore, the motif can be considered *non-consistent*.

Figure 3(c) shows an all-to-all small network in which all edges are weighted by the control parameter α_c. In this case the network topology and the coupling strength distribution make this network more symmetrical. Accordingly, the α_c range for which coexistence exists is narrower with respect to the previous studied motifs. This reduction of the area of coexistence has implications in the consistency of synchronizations: zero-crossings of CLEs, are randomly distributed in a tiny range of α_c and, so, coupled pairs in the network do not consistently lay in the same synchronized state for different initial conditions (see Fig. 3(c) right panel).

Overall, by gathering the results of the coexistence and the consistency phenomena, we show that network symmetries govern the synchronization dynamics emerging from a system of coupled dynamical units.[35] In this regard, clusters of synchronizations dynamically emerge thanks to symmetry breaking (with respect to the topology, the system parameter values, or both) and the statistics of the synchronization dynamics strongly depend on the type of symmetry breaking.

IV. CONSTRUCTION OF CONSISTENT NETWORKS

Functional networks can be constructed by establishing relationships between their (coupled) elements. One of the most prominent dynamical features that functionally relate two oscillators is synchronization, which may take the aforementioned forms (PS, GS, LS, and CS) among others not studied here. Therefore, synchronization is a probe for assessing a (non) trivial relationship between two dynamical systems. In this sense, in contrast to traditional approaches where only one type of synchronization is considered, the statistics of coexistence may reveal a complex functional organization of synchronization within a network and, therefore, may help to construct robust functional networks.

First, the motifs studied in Fig. 3 are coupled through their hubs (or most connected nodes) to construct a larger network of dynamical units. The resulting graph is shown in Fig. 4(a), where each of the motifs is labeled as A, B, or C. The intra-motif weights are the same as the selected in Figs. 3(a)–3(c), respectively, whereas the inter-hub links weights are shown in the caption of Fig. 4. Figure 4(b) shows the statistics of synchronization occurrence in this network: cluster A shows a very robust consistency of its synchronizations whereas clusters B and C are much less consistent, i.e., they display a wide repertoire of different synchronization motifs depending on the initial conditions. However, as can be noticed when comparing the relative-frequency plots shown in Figs. 3(a)–3(c) and 4(b), the dynamics of synchronization is altered when the three motifs are embedded in a larger network. This fact is a signature for assessing that the dynamics of coexistence in the large network is not just the simple juxtaposition of the dynamics of its composite sub-network motifs.

The construction of the functional networks arising from the synchronization patterns in this network is performed as follows: the statistical occurrence of each synchronization among pairs of nodes of the system is taken into account to better characterize the most salient synchronization motifs between the nodes. Then, thresholds in the statistical occurrence of each pairwise synchronization are applied, leading to the extraction of the links which, statistically, appear the most and so are more *consistent*.

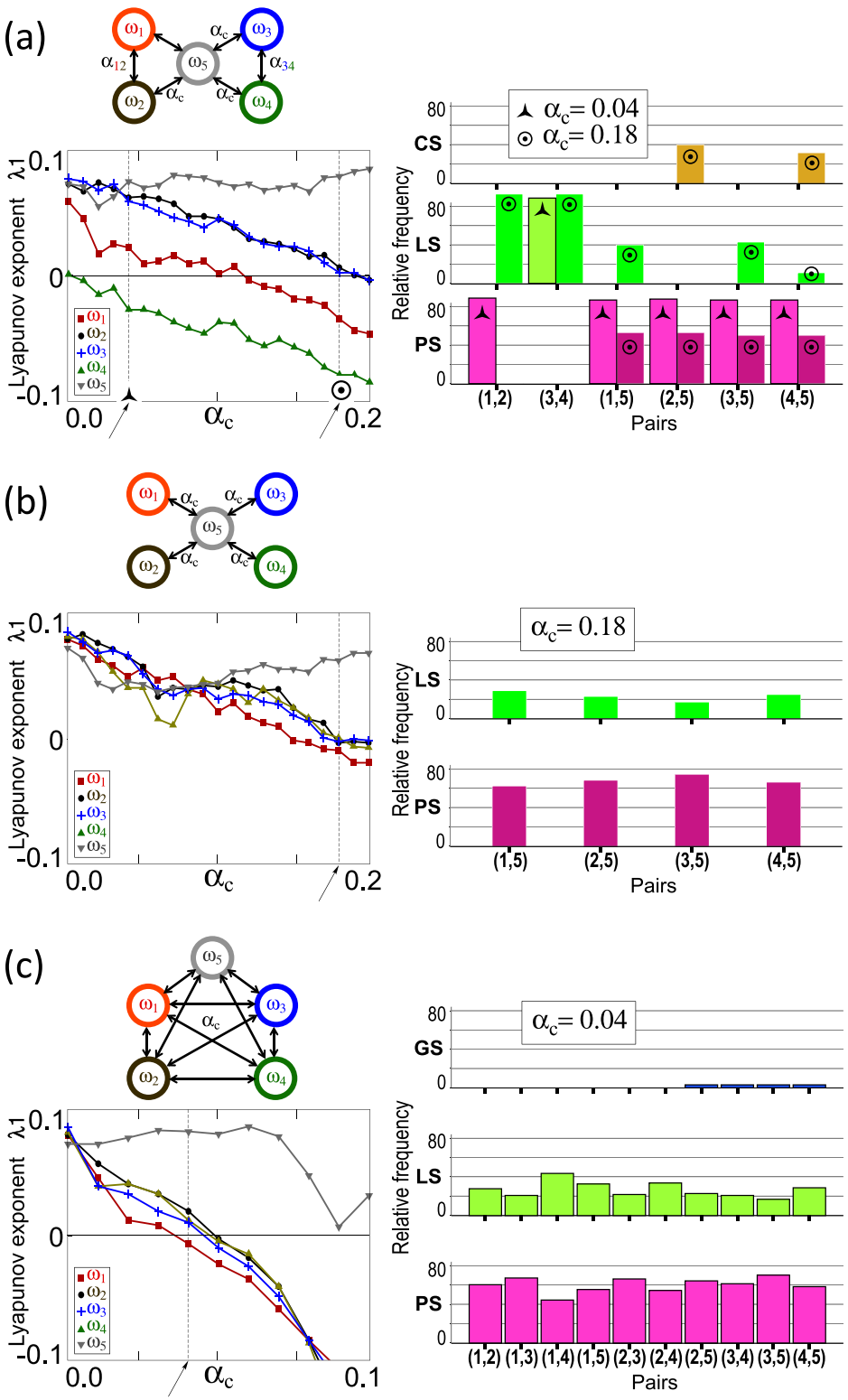

FIG. 3. Consistency of the coexistence of synchronizations. (a) Same network of Fig. 2(a) with coupling $\alpha_{3,4} = 0.20$ for node pair 3–4. For each node dynamics, the curves show the mean value of the maximum Lyapunov exponent ($\lambda 1$) as a function of coupling strength α_c (see Fig. 2(b)). The histogram shows the relative frequency of the synchronization patterns for selected values of α_c ($\alpha_c = 0.04$, $\alpha_c = 0.18$ indicated by the arrows). (b) Homogeneous hub network with all couplings weighted by α_c. The maximum Lyapunov exponent curves for each node dynamics are similar and the interval of α_c for coexistence of synchronization patterns is small. The histogram shows the distribution of the synchronization patterns for $\alpha_c = 0.18$. (c) All-to-all network in which all couplings are weighted by α_c. The interval for coexistence of synchronization patterns is also small and occurs for smaller values of α_c. The histogram shows the distribution of the synchronization patterns for $\alpha_c = 0.04$.

Figure 4(c) shows the construction of the functional network emerging from the structural motif-based network by applying different levels of consistency for each synchronization pattern. For each threshold, this construction takes into account links that show *the same* synchronization a number of times greater than the consistency threshold. Accordingly, the constructed functional network coincides with the most consistent motif (A) rather than with subsystems B and C, which do not show consistent synchronization patterns. However, these non-consistent patterns allow us to infer a homogeneous coupling distribution in these modules, which is also informative about the underlying network structure.

The study of larger networks allows to generalize the relationship between the dynamical features of heterogeneous synchronization patterns with their structural and functional topological characteristics. By taking the SF prototypical network shown in Fig. 1 and performing topological changes—taking clustering as a control parameter—a

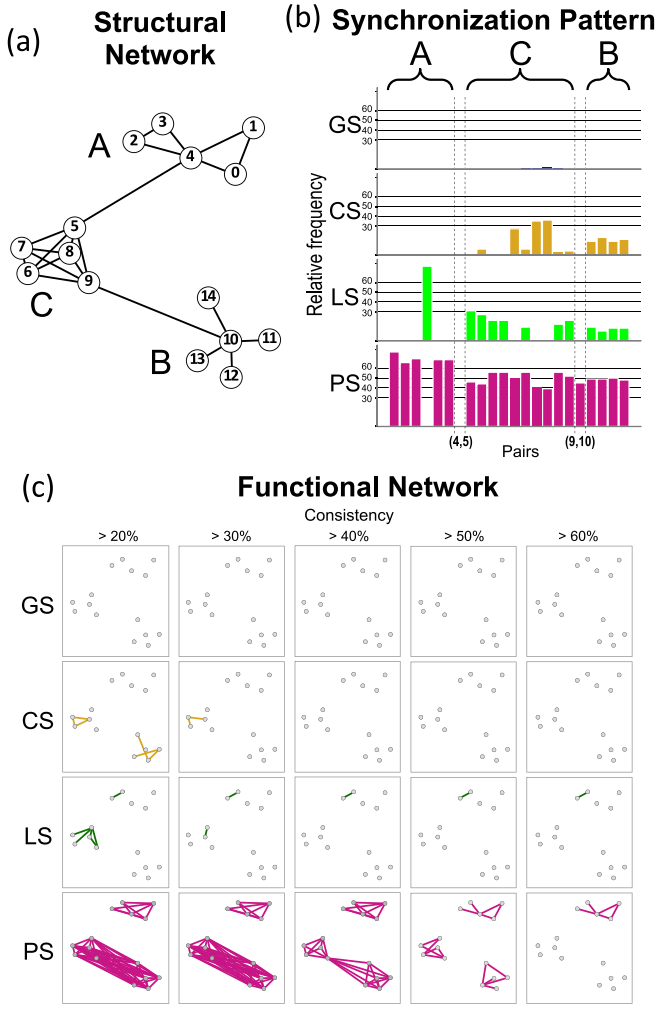

FIG. 4. Construction of functional networks. (a) A structural network of modules is constructed by linking a module A, corresponding to the motif in Fig. 3(a), with a module C, corresponding to the motif in Fig. 3(c), by means of node pair 4–5 with coupling $\alpha_{4,5} = 0.03$ and by linking the module C with a module B, corresponding to the motif in Fig. 3(b), by means of node pair (9, 10) with coupling $\alpha_{9,10} = 0.04$. The internal coupling strengths of the modules are the same as for the isolated motifs in Figs. 3(a)–3(c). (b) Histogram of the relative frequency of the synchronization patterns for all intra-module and for the two intermodule node pairs. Notice that the consistency of synchronization patterns in modules B and C is different from the consistency observed in isolated networks with the same topology corresponding to modules B and C (see Figs. 3(b) and 3(c)). NS is not shown in the histograms. (c) Functional networks can be determined on the basis of various threshold levels of consistency (between 20% and 60%) for each type of synchronization pattern. Here, we propose to consider the coexistence of synchronizations too. In this example, some coupling between elements in B and C can be inferred. The fact that these subsystems are not consistent suggests that the couplings between their elements are highly homogeneous.

potential relationship between network symmetries and the consistency of the synchronization patterns can be unveiled.

Figure 5(a) shows the fraction of connected synchronized pairs in the SF networks whose consistency is above a certain threshold for increasing clustering. Noticeably, only low clustering networks have edges whose synchronization is consistent above a 50% of the realizations, arguably because only low clustering SF networks are heterogeneous enough to hold consistent synchronized dynamics. Figure 5(b) shows an example of a very consistent realization-averaged SF network with clustering $C = 0.15$ and a consistency map displaying the statistics of synchronization for each pair of nodes in the network. According to the statistics, the realization-averaged colors in the network mostly coincide with pure synchronization colors. Figure 5(c) shows a low consistency realization-averaged SF with clustering $C = 0.40$. The consistency map, performed for every pair of nodes in this network, shows no pattern compared with the case in panel (b). Such patterns denote that the functional organization of these networks is robust in the first case, whereas for the network with larger clustering randomized functional relationships are established among pairs of (connected) nodes.

The structure-function relationship can be quantified by calculating the number of coincident structural and functional links (called n_{true} here onwards) and the number of non-coincident structural and functional links (called n_{false} here onwards)

$$n_{true} = \frac{n_c}{n_T}, \tag{6}$$

$$n_{false} = \frac{n_{in}}{n_{a-t-a} - n_T}, \tag{7}$$

where n_T is the number of edges in the structural network, n_{a-t-a} is the number of edges in an equivalent all-to-all network, n_c is the number of constructed edges that belong to the structural network, n_{in} is the number of constructed edges that do not belong to the structural network, n_{true} is the ratio of constructed edges that belong to the structural network, and n_{false} is the ratio of constructed edges that do not belong to the structural network. In other words, n_{true} computes how many of the structural edges have been reconstructed, whereas n_{false} computes how many of the non-structural edges have been reconstructed. Note that the sum $n_{true} + n_{false}$ is not equal to 1 necessarily. In this sense, a construction with high n_{true} and high n_{false} indicates that the constructed network is close to an all-to-all network, i.e., all structural edges can be retrieved but the number of non structural edges is also high, implying a bad matching between structure and function. Figure 5(b) indicates that for clusterings below $C = 0.15$ the matching between structural and functional network is high for a consistency threshold of about 50%, whereas the construction for higher clusterings provides either a high ratio of false positives (close to all-to-all functional network) or non-consistent networks. Interestingly, the system faces a transition point at a relatively low clustering value, $C \simeq 0.21$, which prevents the construction of functional networks at higher clusterings. Indeed, as the heterogeneity in the structural network is progressively lost due to higher clustering, the system loses consistency in the synchronization motifs and so no robust functional relationships can be extracted.

V. CONCLUSIONS

The coexistence of synchronizations is a phenomenon in which a variety of complex functional relationships are established between the dynamical evolutions of some coupled oscillatory elements. Such scenario emerges in the route towards an all-synchronized network, where trivial

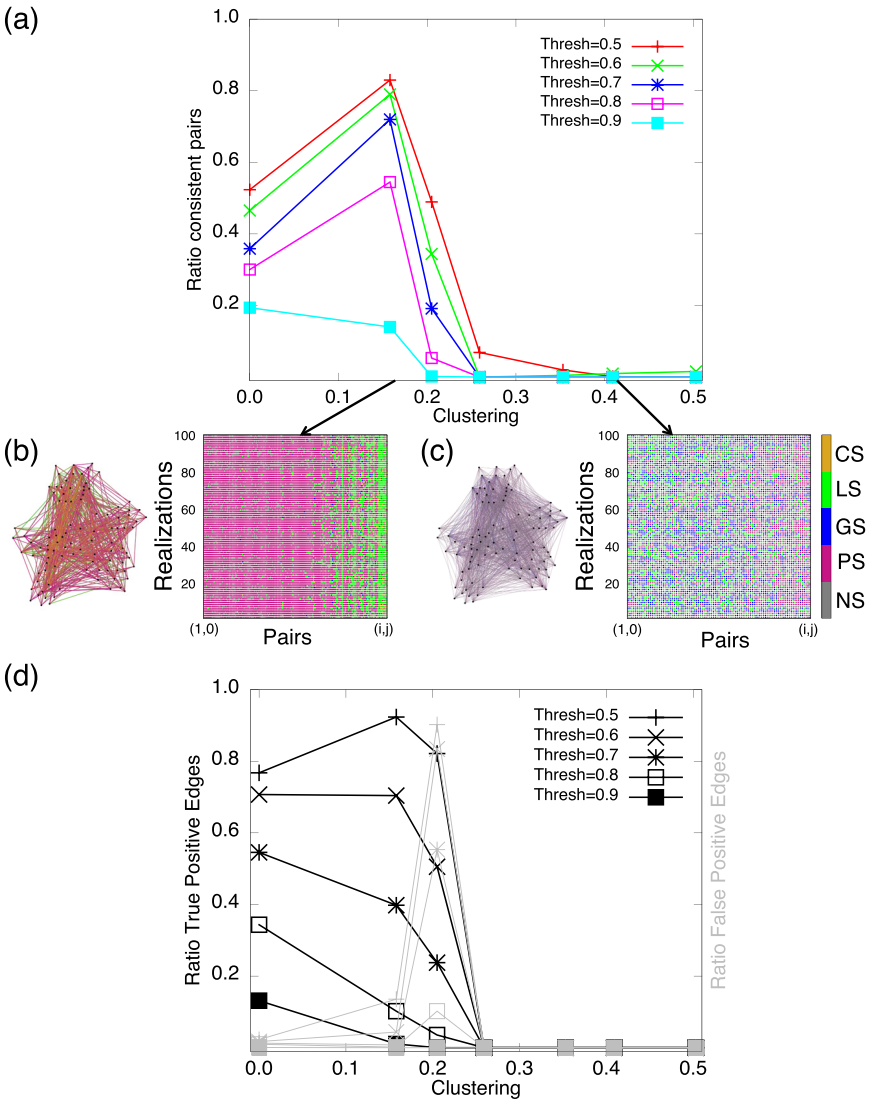

FIG. 5. Relationship between structural and functional networks for increasing clustering. (a) Ratio of consistent pairs for increasing clustering and increasing consistency thresholds (*Thresh*). The ratio of consistent edges displays a maximum for low clustering values, showing the dependence of this feature on the symmetries of the networks. (b) Low clustering networks ($C = 0.15$) show consistent synchronization motifs, as shown in the synchronization-averaged network—which shows almost pure synchronization colors—and in the realization vs. pair synchronization map—which displays patterns of synchronization. (c) For larger clustering networks ($C = 0.40$), the synchronization-averaged networks show a single color and no patterns can be discerned in the realization vs. pair synchronization map. (d) The combination of coexistence and its consistency allows to reconstruct functional networks that embed information of the underlying structural network. The ratio of true and false positive edges for the same networks as in panel A shows that low clustering structural networks can be reconstructed more reliably than higher clustering structural networks. In this regard, heterogeneous networks are more consistent in the synchronization dynamics and so may be easily found, as happens often in the works presented in the literature, when extracting functional networks.

correlations are established among oscillators. Although many patterns of synchronization have been described so far, like *chimera* states or single synchronization clusters, no description of the emergence of diverse amplitude and phase correlations within the same network has been addressed before. Therefore, the conditions for which this phenomenon occurs are given here in terms of the CLEs, providing a notion of the attractiveness of the trajectory defined by one oscillator. The coexistence of synchronizations is prominent when there is a broad separation of CLEs between positive and negative values, taking coupling strength as a control parameter. Besides, breaking the symmetry of a network—the number of nodes' contacts or the coupling strengths—increases the even distribution of CLEs and allows for a broad distribution of synchronization motifs. Therefore, weighted complex networks show much more coexistence than their unweighted counterparts.

What is more, some networks can robustly display the same coexistence patterns regardless of the initial conditions imposed, showing high consistency. Such feature allows to better characterize the stable functional relationships established in the network, which is at the basis of functional network construction. In this sense, we show that the matching between structural and functional networks is high in networks displaying consistent heterogeneous synchronization states.

The consistency of the three prototypical networks shown in Fig. 1 is diverse: while SF networks with low clustering show high consistency, SW and RN networks do not display this feature because in SW or RN networks the number of node contacts fluctuates less. The consistency of the coexistence is a consequence of the heterogeneity of the network: the dynamical heterogeneous synchronization clusters consistently lay in the same heterogeneous synchronization manifolds for any of the initial conditions imposed because the synchronized trajectories are always dominated by the most connected neighbors. Previous research shows that, in unweighted and undirected networks, for certain coupling regimes, there is an optimal matching between structural and functional networks.[13] Here, these results are extended to the case of weighted undirected networks and provide a novel method to extract robust functional relationships. Arguably, the method presented in this work is more restrictive because it relies on the preservation of the same heterogeneous

synchronization patterns, but it provides higher robustness to the constructed functional networks.

The present results, though limited in their scope, also point towards a general feature in the structure-function relationship in network science: the construction of functional networks, for the oscillators used here, bring about heterogeneous (non-symmetrical) networks because they are more consistent. More symmetric or homogeneous networks will appear as inconsistent if coupling is small: only when coupling is large enough to force global synchronization robust symmetrical networks will show up in the constructed functional networks. We believe that this structure-function relationship may also be true for other oscillators. Our result explains some previous experimental results. For instance, in brain dynamics, previous experimental studies have shown that consistent dynamics result in selected network topologies that have been retrieved much more often than others.[36,37] However, further theoretical and experimental studies, for other systems, should address this point to limit or extend the validity of the conclusions raised here.

ACKNOWLEDGMENTS

This work was partially supported by the Spanish Ministry of Economy and Competitiveness and FEDER (Project No. FIS2015-66503). AEPV acknowledges support from the Swiss National Science Foundation Project NEURECA (CR13I1 138032). J.G.O. also acknowledges support from the the Generalitat de Catalunya (Project No. 2014SGR0947), the ICREA Academia Programme, and from the "María de Maeztu" Programme for Units of Excellence in R&D (Spanish Ministry of Economy and Competitiveness, MDM-2014-0370).

[1]A. Pikovsky, M. Rosenblum, and J. Kurths, *Synchronization: A Universal Concept in Nonlinear Sciences* (Cambridge University Press, 2003), Vol. 12.
[2]S. Strogatz, *Sync: The Emerging Science of Spontaneous Order* (Hachette Books, 2003).
[3]S. H. Strogatz, Phys. D: Nonlinear Phenom. **143**, 1 (2000).
[4]L. Glass, Nature **410**, 277 (2001).
[5]D. Abrams and S. Strogatz, Phys. Rev. Lett. **93**, 174102 (2004).
[6]I. Omelchenko, Y. Maistrenko, P. Hövel, and E. Schöll, Phys. Rev. Lett. **106**, 234102 (2011).
[7]C. Yao, M. Yi, and J. Shuai, Chaos **23**, 033140 (2013).
[8]L. M. Pecora, F. Sorrentino, A. M. Hagerstrom, T. E. Murphy, and R. Roy, Nat. Commun. **5**, 4079 (2014).
[9]L. Schmidt, K. Schönleber, K. Krischer, and V. García-Morales, Chaos **24**, 013102 (2014).
[10]E. Schöll, Eur. Phys. J. Spec. Top. **225**, 891 (2016).
[11]M. Chavez, D.-U. Hwang, A. Amann, H. G. E. Hentschel, and S. Boccaletti, Phys. Rev. Lett. **94**, 218701 (2005).
[12]G. Tirabassi, R. Sevilla-Escoboza, J. M. Buldú, and C. Masoller, Sci. Rep. **5**, 10829 (2015).
[13]W. Lin, Y. Wang, H. Ying, Y.-C. Lai, and X. Wang, Phys. Rev. E **92**, 012912 (2015).
[14]B. Blasius, A. Huppert, and L. Stone, Nature **399**, 354 (1999).
[15]P. A. Robinson, J. J. Wright, and C. J. Rennie, Phys. Rev. E **57**, 4578 (1998).
[16]S. Hill and A. Villa, Network: Comput. Neural Syst. **8**, 165 (1997).
[17]J. Cabessa and A. Villa, PLoS One **9**, e94204 (2014).
[18]D. Malagarriga, A. E. P. Villa, J. Garcia-Ojalvo, and A. J. Pons, PLoS Comput. Biol. **11**, e1004007 (2015).
[19]J. I. Deza, M. Barreiro, and C. Masoller, Chaos: Interdiscip. J. Nonlinear Sci. **25**, 033105 (2015).
[20]D. H. Zanette, Europhys. Lett. **68**, 356 (2004).
[21]O. I. Moskalenko, A. A. Koronovskii, A. E. Hramov, and S. Boccaletti, Phys. Rev. E **86**, 036216 (2012).
[22]A. Uchida, F. Rogister, J. García-Ojalvo, and R. Roy, Prog. Opt. **48**, 203–341 (2005).
[23]L. Xiao-Wen and Z. Zhi-Gang, Commun. Theor. Phys. **47**, 265 (2007).
[24]M. G. Rosenblum, A. S. Pikovsky, and J. Kurths, Phys. Rev. Lett. **76**, 1804 (1996).
[25]H. Abarbanel, N. Rulkov, and M. Sushchik, Phys. Rev. E **53**, 4528 (1996).
[26]M. G. Rosenblum, A. S. Pikovsky, and J. Kurths, Phys. Rev. Lett. **78**, 4193 (1997).
[27]S. Boccaletti, J. Kurths, G. Osipov, D. Valladares, and C. Zhou, Phys. Rep. **366**, 1 (2002).
[28]J. P. Lachaux, E. Rodriguez, J. Martinerie, and F. J. Varela, Hum. Brain Mapp. **8**, 194 (1999).
[29]O. Rössler, Phys. Lett. A **57**, 397 (1976).
[30]P. Erdős and A. Rényi, Publ. Math. (Debrecen) **6**, 290 (1959).
[31]D. J. Watts and S. H. Strogatz, Nature **393**, 440 (1998).
[32]A.-L. Barabási and R. Albert, Science **286**, 509 (1999).
[33]K. Jittorntrum, J. Optim. Theory Appl. **25**, 575 (1978).
[34]I. Leyva, R. Sevilla-Escoboza, J. M. Buldú, I. Sendiña Nadal, J. Gómez-Gardeñes, A. Arenas, Y. Moreno, S. Gómez, R. Jaimes-Reátegui, and S. Boccaletti, Phys. Rev. Lett. **108**, 168702 (2012).
[35]V. Nicosia, M. Valencia, M. Chavez, A. Díaz-Guilera, and V. Latora, Phys. Rev. Lett. **110**, 174102 (2013).
[36]V. M. Eguíluz, D. R. Chialvo, G. a. Cecchi, M. Baliki, and A. V. Apkarian, Phys. Rev. Lett. **94**, 018102 (2005).
[37]E. Bullmore and O. Sporns, Nat. Rev. Neurosci. **10**, 186 (2009).